# GENERATION OF PHOTON-NUMBER-SQUEEZED LIGHT BY SEMICONDUCTOR INCOHERENT LIGHT SOURCES

Malvin C. Teich
Columbia University

Bahaa E. A. Saleh
University of Wisconsin

Federico Capasso
AT&T Bell Laboratories

Reprinted from
Coherence, Amplification, and Quantum Effects in Semiconductor Lasers
Chapter No. 12

# 12

# Generation of Photon-Number-Squeezed Light by Semiconductor Incoherent Light Sources

MALVIN C. TEICH
*Columbia Radiation Laboratory, Columbia University, New York, New York*

BAHAA E. A. SALEH
*Department of Electrical and Computer Engineering, University of Wisconsin, Madison, Wisconsin*

FEDERICO CAPASSO
*AT&T Bell Laboratories, Murray Hill, New Jersey*

## 12.1. INTRODUCTION

Photon-number-squeezed light, by definition, exhibits a photon-number uncertainty that is squeezed below the minimum classical value, which is associated with the Poisson distribution [1, 2]. Such light is therefore also called sub-Poisson light. Photon-number-squeezed light is expected to find use in a variety of applications, ranging from lightwave communications [3, 4] to biology [5], where the capacity of light to carry information is limited by photon-number uncertainty. Indeed, the use of a fixed number of photons to represent a bit of information can, in principle, provide noise-free direct-detection lightwave communications [3, 4]. The noise is squeezed into the phase fluctuations, which are not registered by the process of direct detection.

Photon-number-squeezed light may be generated in many ways. When it is desired to impart information on the phase of a light beam, the use of

*Coherence, Amplification, and Quantum Effects in Semiconductor Lasers*, Edited by Yoshihisa Yamamoto.
ISBN 0-471-512494 

quadrature-squeezed light [6, 7] that is mixed with coherent light at a beamsplitter [8] is particularly useful. The homodyne process converts the quadrature-squeezed light into photon-number-squeezed light [9]. The distinction between quadrature-squeezed and photon-number-squeezed light has been elucidated elsewhere [2, 10, 11].

Techniques in which photon-number-squeezed light is directly generated are sometimes preferable because of their simplicity. Such techniques are useful when information is to be imparted directly to the photon number. Yamamoto and his colleagues have considered several schemes that in principle permit the synthesis of light with a particular quantum state [10]; these include unitary transformation from a coherent state, nonunitary state reduction by measurement, the combination of measurement and feedback, and lasing with suppressed pump-noise fluctuations. The latter approach is considered in the context of semiconductor injection lasers in the previous chapter of this book [11].

An alternative approach, initially used by us [1, 12] and considered in this chapter, focuses on the point process that characterizes the generation and detection of photons in terms of their arrival times. It is most readily applied to a description of incoherent photon-number-squeezed light. This approach is meritorious in the physical intuition that it provides and the fact that it includes time dynamics, but it does not provide a framework that allows for the synthesis of light of a particular quantum state.

Most sources of laser light produce a statistically independent stream of photons represented by the Poisson point process. The generation of photon-number-squeezed light requires that anticorrelations be introduced into the photon stream. These anticorrelations may be manifested in the times at which the radiators emit photons (excitation control) or they may be derived from the emitted photons themselves (photon control) [1, 2].

In this chapter, we focus on the generation of photon-number-squeezed light by techniques that rely on excitation control (Section 12.2). Excitation control may be imparted by mechanisms that rely either on a physical process (Section 12.3), or on an externally provided feedback control signal (Section 12.4). Both of these techniques can be used in conjunction with semiconductor light sources. Two proposed applications of photon-number-squeezed light are briefly considered in Section 12.5. An analysis of the generation of photon-number-squeezed light from a stochastic point process point of view is detailed in the Appendix.

In principle, these techniques can be used to generate ideal photon-number-state light (which has no uncertainty in its photon number). However, it is important to note that photon-number squeezing is a fragile effect. Once produced it is readily diluted by the ever-present random loss of photons and by contamination arising from the presence of (unsqueezed) background photons [1, 13].



## 12.2. EXCITATION CONTROL

The generation of photon-number-squeezed light by excitation control may be visualized in terms of the schematic representation shown in Figure 12.1. Two key effects regulate the photon-number-squeezing possibilities for light generated by a two-step process of excitation and emission: (1) the statistical properties of the excitations themselves and (2) the statistical properties of the individual emissions. The role of these two factors is heuristically illustrated in Figure 12.1 and analytically examined in the Appendix (which is drawn from Section 3.4 of Ref. 1).

In Figure 12.1*a*, we show an excitation process that is Poissonian. Consider each excitation as generating photons independently. Now if each excitation instantaneously produces a single photon, and if we ignore the effects of interference, the outcome is a Poisson stream of photons, which is obviously not sub-Poisson. This is the least random situation that we could hope to produce, given the Poisson excitation statistics. If interference is present, it will redistribute the photon occurrences, leading to the results for chaotic light [14]. On the other hand, the individual nonstationary emissions may consist of multiple photons or random numbers of photons. In this case, we encounter two sources of randomness, one associated with the excitations and another associated with the emissions. The outcome will then be super-Poisson; that is, it will exhibit photon-number fluctuations greater than those associated with the Poisson distribution.

In particular, if the emissions are also described by Poisson statistics, and the counting time is sufficiently long, the result turns out to be the Neyman Type-A counting distribution, as has been discussed in detail elsewhere [15, 16]. Even if the individual emissions comprise deterministic numbers of photons, the end result is the fixed-multiplicative Poisson distribution, which is super-Poisson [16]. Related results have been obtained when interference is permitted [14]. It is quite clear, therefore, that if the excitations themselves are Poisson (or super-Poisson), there is no hope of generating photon-number-squeezed light by such a two-step process.

In Figure 12.1*b* we consider a situation in which the excitations are more regular than Poisson. For illustration and concreteness, we choose the excitation process to be produced by deleting every other event of a Poisson pulse train. The outcome is the gamma-2 (or Erlang-2) renewal process, whose analytical properties are well understood (see Appendix). Single-photon emissions, in the absence of interference, result in sub-Poisson photon statistics. Poisson emissions, on the other hand, result in super-Poisson light statistics. Of course, the presence of interference can introduce additional randomness. Clearly, a broad variety of excitation processes can be invoked for generating many different kinds of light. A

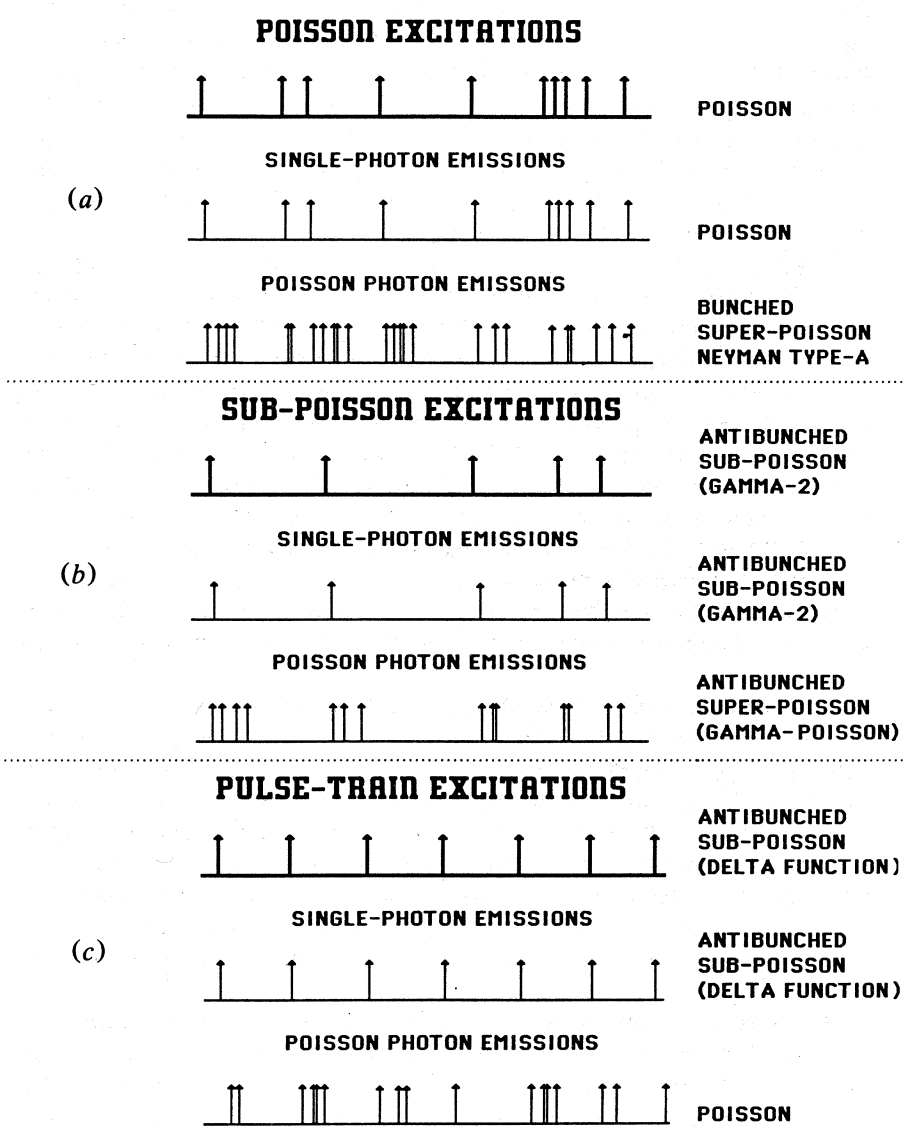


**Figure 12.1.** Schematic representation of a two-step process for the generation of light, illustrating stochastic excitations (first line) with either single-photon emissions (second line) or Poisson multiple-photon emissions (third line). Interference effects are ignored in this simple representation. (*a*) Poisson excitations; (*b*) sub-Poisson, antibunched excitations (gamma-2); (*c*) pulse-train excitations (random phase). After Teich et al. [12].



process similar to the gamma-2, and for which many analytical results are available, is the nonparalyzable dead-time-modified Poisson process (see Appendix). Resonance fluorescence radiation from a single atom is described by a process of this type since, after emitting a single photon, the atom decays to the ground state, where it remains for a period of time and cannot radiate. Short and Mandel used such a scheme to produce conditionally photon-number-squeezed emissions from isolated atoms [17].

Finally, in Figure 12.1*c*, we consider the case of pulse-train excitations (with random initial time). This is the limiting result both for the gamma family of processes and for the dead-time-modified Poisson process. In the absence of interference, single-photon emissions in this case yield ideally sub-Poisson photon statistics. Interference does not destroy the sub-Poisson nature in the long-counting-time limit. Poisson emissions give rise to Poisson photon statistics.

The illustration presented in Figure 12.1 is intended to emphasize the importance of the excitation and emission statistics as determinants of the character of the generated light. To produce sub-Poisson photons by direct generation, both sub-Poisson excitations and sub-Poisson emissions are required.

The statistical properties of light generated by sub-Poisson excitations, with each excitation leading to a single-photon emission, has been examined in considerable detail by Teich et al. [12]. These authors also addressed the effects of different locations for the different emissions and the rates of photon coincidence at pairs of positions in the detection plane. Some of the results are summarized in the Appendix.

The sub-Poisson excitations are characterized by a time constant $\tau_e$ that represents the time over which excitation events are anticorrelated (antibunched). The single-photon emissions, on the other hand, are characterized by a photon excitation–emission lifetime $\tau_p$. The detected light will be photon-number-squeezed provided $T \gg \tau_e, \tau_p$; $A \gg A_c$, where $T$ is the detector counting time, $A$ is the detector counting area, and $A_c$ is the coherence area. Different methods of sub-Poisson excitation result in different values of $\tau_e$ whereas different mechanisms of photon generation result in different values of $\tau_p$ and $A_c$.

Invoking these limits assures that all memory of the fields from individual emissions lie within the detector counting time and area, in which case the randomization of photon occurrences associated with interference does not extend beyond these limits. Consequently, the photon-counting statistics are determined by the only remaining source of variability, which is the randomness in the excitation occurrences. In this limit the photons behave as classical particles.

To recapitulate, a stationary stream of photon-number-squeezed light can be generated by a two-step process if sub-Poisson statistics are obeyed both by the excitations and by the individual emissions. For sufficiently large counting times and large detection areas, interference effects are

washed out and the photons behave as classical particles. If the emissions are single photons, the overall photon statistics then directly mimic the statistics of the excitations.

This result is applicable even for physical processes that operate on the basis of nonindependent emissions as long as the counting time and area are sufficiently large in comparison with the time and area over which dependent emissions occur. Thus our approach is useful for understanding the generation of photon-number-squeezed light by incoherent sources, as described in this chapter, and by devices such as semiconductor lasers as described in the previous chapter [11].

## 12.3. EXCITATION CONTROL PROVIDED BY A PHYSICAL PROCESS

We now consider several excitation control methods that make use of the sub-Poisson excitations inherent in space-charge-limited current flow. Such a current is naturally sub-Poisson as a result of the intrinsic Coulomb repulsion of the flowing electrons. In this case the excitation control results from a physical process.

Coulomb repulsion, which is the underlying physical process responsible for space-charge-limited current flow, is ubiquitous when excitations are achieved by means of charged particle beams. The single-photon emissions may be obtained in any number of ways. Three examples are provided: In Section 12.3.1 (which serves as the prototype for the following subsections) they arise from spontaneous fluorescence emissions in Hg vapor, in Section 12.3.2 they represent spontaneous recombination photons in a semiconductor, and in Section 12.3.3 they are stimulated recombination photons in a semiconductor. These methods all generate photon-number-squeezed light by transferring the anticlustering properties of the electrons, ultimately arising from Coulomb repulsion, directly to the photons.

### 12.3.1. Space-Charge-Limited Franck–Hertz Experiment

The space-charge-limited Franck–Hertz effect [18–20] provided the first source of unconditionally photon-number-squeezed light. The essential element of this experiment is a collection of Hg atoms excited by inelastic collisions with a low-energy space-charge-limited ("quiet") electron beam. The space-charge reduction of the usual shot noise associated with thermionically emitted electrons can be substantial [21, 22]. A convenient measure of the noise reduction is provided by the Fano factor, which is defined as the ratio of the variance $\mathrm{Var}(m)$ to the mean $\langle m \rangle$ of a random variable: $F_m \equiv \mathrm{Var}(m)/\langle m \rangle$. Fano factors for the electron stream with values $F_e < 0.1$ are typical, and values as low as 0.01 are possible. After

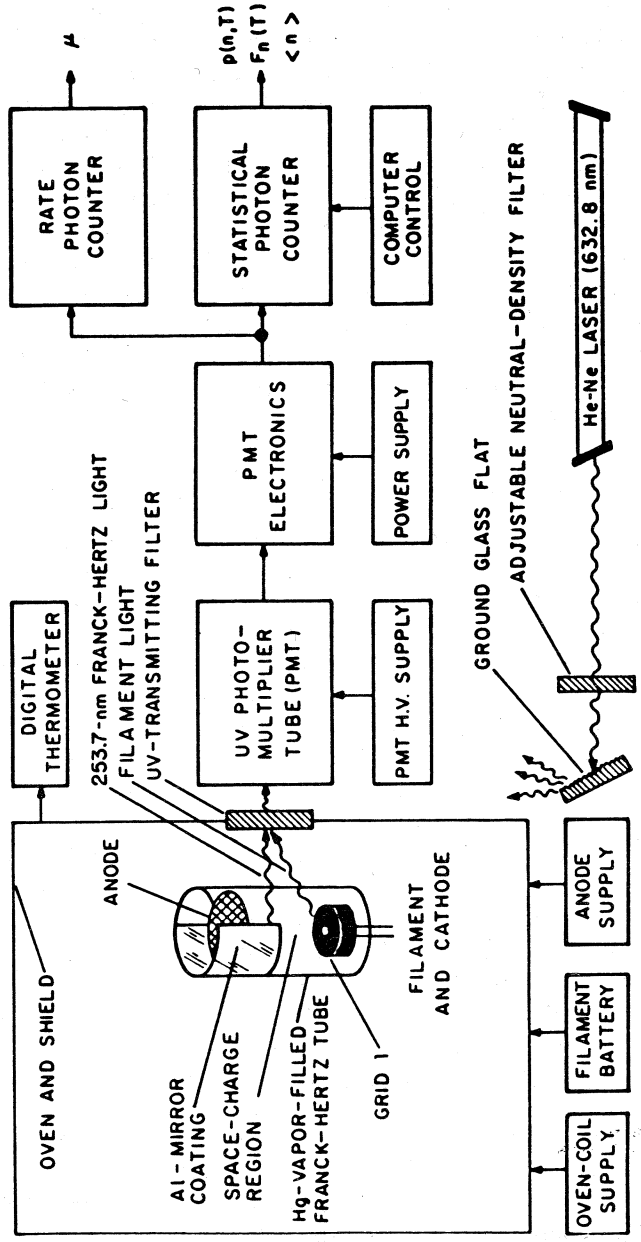


**Figure 12.2.** Block diagram of the space-charge-limited Franck–Hertz experiment. The use of Hg resulted in ultraviolet photon-number-squeezed light at a wavelength of 253.7 nm. After Teich and Saleh [20].

excitation, each atom emits a (sub-Poisson) single photon via the Franck–Hertz (FH) effect.

A block diagram of apparatus originally used to carry out this experiment is shown in Figure 12.2. The light was generated in a specially constructed 25-mm-diameter UV-transmitting Franck–Hertz tube, filled with 0.75 g of Hg. The radiation impinged on a UV photon-counting photomultiplier tube (PMT) in a special base that provided preamplification, discrimination, and pulse shaping. The output of this circuitry was fed to electronic photon-counting equipment that measured the probability distribution $p(n, T)$ for the detection of $n$ photoelectrons in time $T$. The mean count $\langle n \rangle$ and the Fano factor $F_n(T)$ were calculated from $p(n, T)$. The photon count was only slightly sub-Poisson, but the result was statistically significant. The small degree of photon-number squeezing resulted principally from optical losses in the experimental apparatus. The details of the experiment and the experimental results have been described elsewhere [19, 20].

### 12.3.2. Space-Charge-Limited Excitation of Recombination Radiation

A useful source of photon-number-squeezed light should exhibit a photon Fano factor that is substantially below unity while producing a large photon flux, preferably in a directed beam. It should also be small in size and rapidly switchable.

This has led us to propose a semiconductor device structure in direct analogy with the Franck–Hertz experiment described above. Sub-Poisson electron excitations are attained through space-charge-limited current flow and single-photon emissions are achieved by means of recombination radiation [23]. A device of this nature will emit incoherent photon-number-squeezed recombination radiation and should be far more efficient than its vacuum-tube cousin. The energy-band diagram for such a space-charge-limited light-emitting device (SCLLED) is illustrated in Figure 12.3. Sub-Poisson electrons are directly converted into sub-Poisson photons, as in the space-charge-limited Franck–Hertz experiment, but these are now recombination photons in a semiconductor. In designing such a device, carrier and photon confinement should be optimized and optical losses should be minimized. The basic structure of the device is that of a $p^+$–$i$–$n^+$ diode. Recombination radiation is emitted from the LED-like region.

The current noise in such a space-charge-limited diode [24] can be quite low. It has a thermal (rather than shot-noise) character [25–27]. The current noise spectral density $S_e(\omega)$ for a device in which only electrons participate in the conduction process is given by [23]

$$\frac{S_e(\omega)}{2e\langle I_e \rangle} = \frac{8k\theta}{e\langle V_e \rangle} \tag{12.1}$$



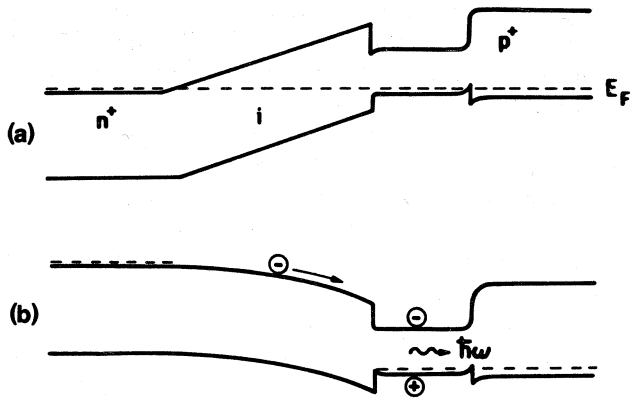


**Figure 12.3.** Energy-band diagram of a specially designed solid-state space-charge-limited light-emitting device under (*a*) equilibrium conditions and (*b*) strong forward-bias conditions. The curvature of the intrinsic region under forward-bias conditions indicates the space-charge potential. After Teich et al. [23].

where $\langle I_e \rangle$ is the average forward current in the device, $\langle V_e \rangle$ is the applied forward-bias voltage, $k$ is Boltzmann's constant, $\theta$ is the device temperature in kelvins, $\omega$ is the angular frequency, and $e$ is the electronic charge.

The degree of photon-number squeezing of the detected photons is then expected to be given by [23]

$$F_n(T) = 1 + \eta\left(\frac{8k\theta}{e\langle V_e \rangle} - 1\right) \tag{12.2}$$

provided that background light is absent. For a space-charge-limited diode, such as that shown in Figure 12.3, it is estimated that $8k\theta/e\langle V_e \rangle \approx 0.1$ when $\theta = 300$ K and $\langle V_e \rangle = 2$ V (corresponding to $\langle I_e \rangle \approx 33$ mA). This ratio can be further reduced by cooling the device. If a dome-shaped surface-emitting GaAs/AlGaAs configuration and a Si $p$–$i$–$n$ photodetector are used, the overall quantum efficiency is estimated to be $\eta \approx 0.113$, yielding an overall estimated postdetection Fano factor $F_n(T) \approx 0.90$. A commercially available standard LED should provide $F_n(T) \approx 0.97$. In both cases, $T$ can be as short as $\approx 1$ ns. In principle, the degree of photon-number squeezing of the recombination radiation from the SCLLED is limited only by the geometrical collection efficiency.

### 12.3.3. Sub-Poisson Excitations and Stimulated Emissions

The properties of the light generated by the SCLLED could be improved if stimulated emissions were permitted. The advantages include improved beam directionality, switching speed, spectral properties, and coupling to an optical fiber. This could be achieved by use of an edge-emitting (rather

than surface-emitting) LED configuration, with its waveguiding geometry and superfluorescence properties (single-pass stimulated emission). The theoretical results associated with the simple model presented in Section 12.2 (see Appendix) will apply provided that $T \gg \tau_e, \tau_c$; $A \gg A_c$, where $\tau_c$ and $A_c$ are now the coherence time and coherence area of the superfluorescent emission, respectively. The effect of the stimulated emissions is to extend $\tau_p$ into $\tau_c$ and to reduce the coherence area $A_c$. From a physical point of view, the photons still behave as classical particles in this regime since each electron gives rise to a single photon and there is no memory beyond the counting time $T$.

There will likely be further advantage in combining space-charge-limited current injection with a semiconductor laser structure rather than with the LED structure considered above. This could provide increased emission efficiency as well as additional improvement in beam directionality, switching speed, spectral properties, and coupling. This will be beneficial when the laser can be drawn into a realm of operation in which it produces a state that exhibits photon-number squeezing [28], such as a number-phase minimum uncertainty state [10, 11, 29]. Yamamoto and his colleagues [30, 31] have shown that this mode of operation can be attained in a semiconductor laser oscillator, within the cavity bandwidth and at high photon-flux levels, but in their case the pump fluctuations are suppressed below the shot-noise level by means of externally provided excitation control (see Section 12.4.4). Suggestions of this kind have also been made by Smirnov and Troshin [32] and by Carroll [33].

## 12.4. EXTERNALLY PROVIDED EXCITATION CONTROL

External mechanisms can also be used to ensure that the current flowing in a circuit is sub-Poisson. These include both optoelectronic and current-stabilization schemes. In Section 12.4.1 we discuss the use of two schemes that rely on the use of a light source and photodetector in a negative-feedback loop. The use of a beamsplitter to extract a portion of these in-loop photons is not useful for producing photon-number-squeezed light, as discussed in Section 12.4.2.

In Section 12.4.3 we discuss the possibility of generating sub-Poisson photons from sub-Poisson electrons by making use of an externally provided feedback control signal and an in-loop auxiliary optical source. Sub-Poisson electrons flow through the auxiliary source and produce sub-Poisson photons en route. Finally, in Section 12.4.4 we discuss the generation of sub-Poisson electrons by means of a purely electronic scheme, external current stabilization.

### 12.4.1. Optoelectronic Generation of Sub-Poisson Electrons

Two optoelectronic experiments incorporating externally provided excitation control have been used to generate sub-Poisson *electrons*. One of these was carried out by Walker and Jakeman [34]; the other, by Machida and Yamamoto [35, 36]. The simplest form of the experiment carried out by Walker and Jakeman is illustrated in Figure 12.4. The registration of a photoevent at the detector operates a trigger circuit that causes an optical gate to be closed for a fixed period of time $\tau_d$ following the time of registration. During this period, the power $P_t$ of the (He–Ne) laser illuminating the detector is set precisely equal to zero so that no photoevents are registered. This is a dead-time optical gating scheme. Sub-Poisson photoelectrons were observed.



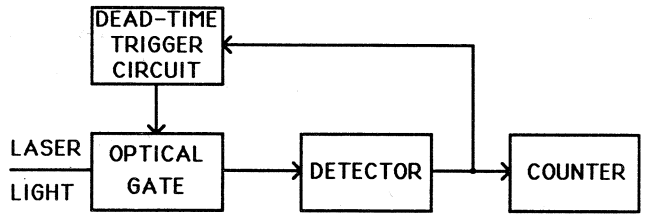


**Figure 12.4.** Generation of sub-Poisson and antibunched electrons by external feedback, as studied by Walker and Jakeman [34].

Machida and Yamamoto's experiment [35] has a similar thrust, although it is based on rate compensation. They used a single-longitudinal-mode GaAs/AlGaAs semiconductor injection laser to generate light (LD) and a Si $p$–$i$–$n$ photodiode (PD) to detect it, as shown in Figure 12.5*a*. Negative feedback from the detector was provided to the current driving the laser diode. A sub-shot-noise spectrum and sub-Poisson photoelectron counts were observed.

The similarity in the experimental results reported by Walker and Jakeman and by Machida and Yamamoto can be understood from a physical point of view [37]. In the configuration used by the latter authors, the injection-laser current (and therefore the injection-laser light output) is reduced in response to peaks of the in-loop photodetector current $i_t$. This rate compensation is essentially the same effect as that produced in the Walker–Jakeman experiment where the He–Ne laser light output is reduced (in their case to zero) in response to photoevent registrations at the in-loop photodetector. The feedback acts like a dead time, suppressing the emission of light in a manner that is correlated with photoevent occurrences at the in-loop detector.

### 12.4.2. Extraction of In-Loop Photons by a Beamsplitter

These simple configurations cannot generate usable sub-Poisson *photons* since the feedback current is generated from the annihilation of the in-loop photons. Any attempt to remove in-loop photons by means of a beamsplitter (BS), such as that illustrated in Figure 2.5*b*, will lead to

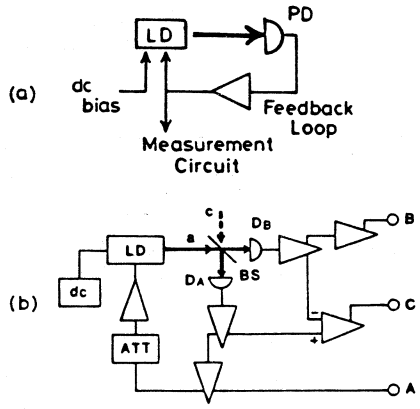


**Figure 12.5.** (*a*) Generation of sub-Poisson and antibunched electrons by external feedback using rate compensation, as investigated by Machida and Yamamoto [35]. (*b*) The removal of in-loop photons by a beamsplitter leads to super-Poisson light at the out-of-loop detector ($D_B$). After Machida and Yamamoto [35].

super-Poisson light. This result can be understood in terms of the arguments of Walker and Jakeman [34] and Shapiro and coworkers [37, 38] and is confirmed by the experiments of Walker and Jakeman [34].

Nevertheless, under special circumstances, and when components other than beamsplitters are used, the feedback technique can be useful in generating photon-number-squeezed light. These involve the use of quantum-nondemolition measurements and correlated photon pairs [1, 38].

### 12.4.3. Use of an In-Loop Auxiliary Optical Source

One of the more direct ways of producing photon-number-squeezed light from a system making use of external feedback is to insert an auxiliary optical source in the path of the sub-Poisson electron stream, as suggested by Capasso and Teich [39]. Two alternative configurations are shown in Figure 12.6. The character of the photon emitter is immaterial; it has been chosen to be an LED for simplicity but it could be a laser. In Figure 12.6*a* the photocurrent derived from the detection of light is negatively fed back to the LED input. It has been established both experimentally [35] and theoretically [37] that, in the absence of the block labeled "source," sub-Poisson electrons (i.e., a sub-shot-noise photocurrent) will flow in a circuit such as this. This conclusion is also valid in the presence of this block, which in this case acts simply as an added impedance to the electron flow.

Incorporating this element into the system offers access to the loop and permits the sub-Poisson electrons flowing in the circuit to be converted into sub-Poisson photons by means of electronic transitions. This is achieved by replacing the detector used in the feedback configurations of Machida and Yamamoto [35] and Walker and Jakeman [34] with a structure that acts simultaneously as a detector and a source. The sub-Poisson electrons emit sub-Poisson photons and continue on their way. The



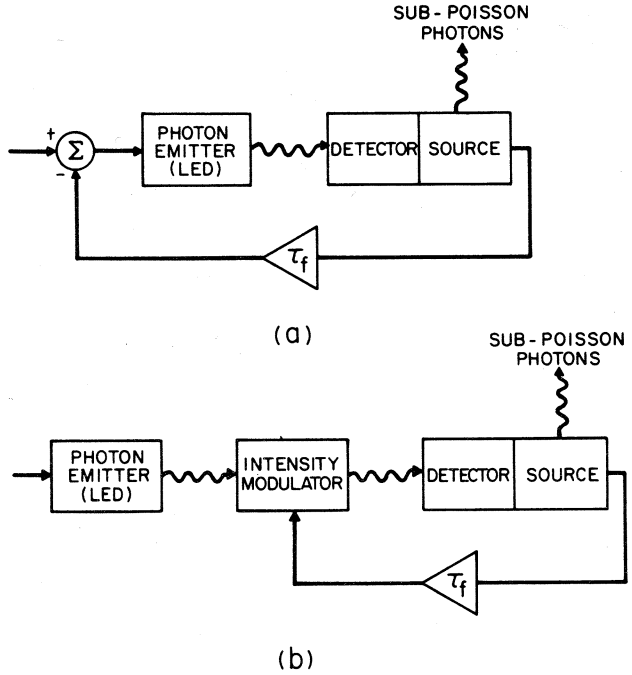


**Figure 12.6.** Generation of photon-number-squeezed light by insertion of an auxiliary source into the path of a sub-Poisson electron stream, as proposed by Capasso and Teich [39]. Wavy lines represent photons; solid lines represent the electron current ($\tau_f$ signifies the feedback time constant). The schemes represented in (*a*) and (*b*) make use of the sub-Poisson electron production methods illustrated in Figures 12.5 and 12.4, respectively. After Capasso and Teich [39].

configuration presented in Figure 12.6*b* is similar except that the (negative) feedback current gates the light intensity at the output of the LED in the manner of Walker and Jakeman, rather than the current at its input in the manner of Machida and Yamamoto. Any similar scheme, such as selective deletion [1, 40], could be used instead.

Two possible solid-state detector–source configurations have been suggested [39]. The scheme shown in Figure 12.7*a* makes use of sequential resonant tunneling [41] and single-photon dipole electronic transitions between the energy levels of a quantum-well heterostructure. The device consists of a reverse-biased $p^+$–$i$–$n^+$ diode where the $p^+$ and $n^+$ heavily doped regions have a wider band gap than the high-field, light-absorbing/emitting $i$ region. This arrangement ensures both high quantum efficiency at the incident photon wavelength (to which the $p^+$ window layer is transparent) and high collection efficiency (due to the waveguide geometry) for the light generated by the electrons drifting in the $i$ layer. An edge-emitting geometry is therefore appropriate. To maximize the

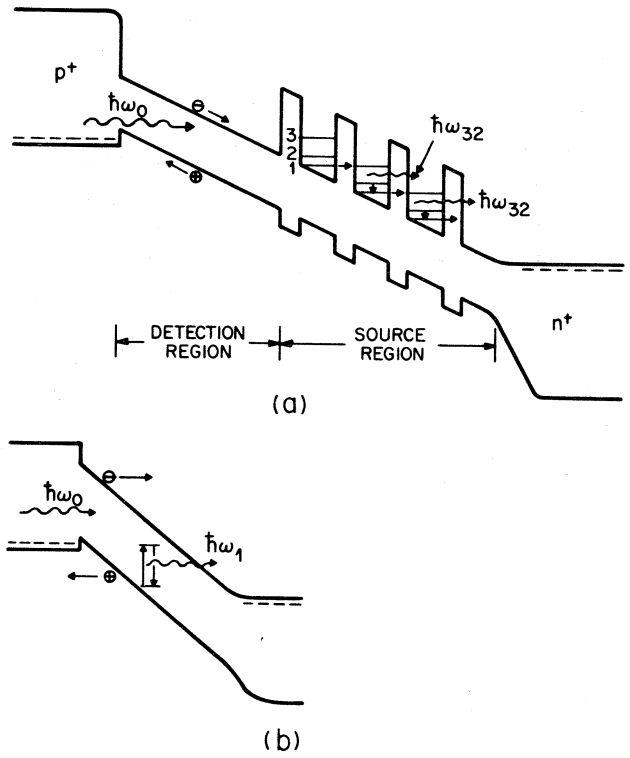


**Figure 12.7.** (*a*) Representative energy-band diagram of a quantum-well detector–source device (see Figure 12.6). The energy of the incident photon emitted by the LED is denoted $\hbar\omega_0$. Detection and source regions are shown. Photons of energy $\hbar\omega_{32}$ are emitted via electronic quantum-well transitions. (*b*) Representative energy-band diagram of a detector–source device with electroluminescent centers impact-excited by energetic photoelectrons, emitting photons with energy $\hbar\omega_1$. After Capasso and Teich [39].

collection efficiency, some of the facets of the device could be reflectively coated. The scheme shown in Figure 12.7*b* is similar except that it uses the impact excitation of electroluminescent centers in the *i* region by drifting electrons. Of course, the ability of configurations such as these to generate photon-number-squeezed light requires the usual interrelations among the various characteristic times associated with the system.

An estimate of the degree to which this mechanism will give rise to photon-number-squeezed light is provided by the Fano factor. The relevant relations are similar to those for the Franck–Hertz source. However, in this situation a single electron may give rise to multiple photons since there are $u$ stages of the device (see Appendix). Numerical estimates for the Fano factor turn out to be similar for both structures illustrated in Figure 12.7, namely, $F_n \approx 0.97$ (under the assumption that the photodetector has an efficiency of 0.8). This is not as good as the value attainable by the SCLLED, principally because of low radiative efficiency in the tunneling scheme. Furthermore the external feedback mechanism may well be slower than the internal feedback scheme of the SCLLED.



### 12.4.4. Use of a Current Source with External Compensation

Steady-state current stabilization can be achieved by use of a constant voltage source in series with an external resistor $R$ [29], or in series with some other optoelectronic component with suitable $I$–$V$ characteristic.

Strong photon-number-squeezed light has been generated in two experiments that make use of external compensation. Tapster *et al.* [42] carried out an elegantly simple experiment, using a high-efficiency commercial GaAs LED fed by a Johnson-noise-limited high-impedance current source. They achieved a Fano factor $F_n \approx 0.96$ over a bandwidth of about 100 kHz, with a current transfer efficiency in excess of 11%. Machida *et al.* [30] fed an InGaAsP/InP single-longitudinal-mode distributed-feedback laser oscillator, operating at a wavelength of 1.56 $\mu$m, with a current source whose fluctuations were suppressed by the use of an external high-impedance element. In their first experiments, these authors obtained an average Fano factor $F_n \approx 0.96$ over a bandwidth of about 100 MHz, with a minimum Fano factor $F_n \approx 0.93$. They calculated that the radiation produced by their device is in a near number-phase minimum-uncertainty state, in the frequency range below the cavity bandwidth (which is in excess of 100 GHz for a typical semiconductor laser). Further results, which are indeed impressive, have been reported more recently [11, 31].

## 12.5. APPLICATIONS

We consider two specific examples where the use of photon-number-squeezed light might prove beneficial. In an idealized direct-detection lightwave communication system, errors (misses and false alarms) can be caused by noise from many sources, including photon noise intrinsic to the light source [1, 3]. If photon noise is the limiting factor, the use of photon-number-squeezed light in place of coherent light can bring about a reduction in this noise, and thereby the probability of error. For a coherent source each pulse of light (which carries a bit of information) contains a Poisson number of photons so that the photon-number standard deviation $\sigma_n = \langle n \rangle^{1/2}$. For photon-number-squeezed light, each pulse contains a sub-Poisson number of photons so that $\sigma_n < \langle n \rangle^{1/2}$. This noise reduction results in a decrease of the error probability. In a simple binary on–off-keying system whose only source of noise is assumed to be binomial photon counts (with Fano factor $F_n$), the mean number of photons per bit $\langle n' \rangle$ required to achieve an error probability of $10^{-9}$ decreases below its

coherent-light "quantum limit" of 10 photons/bit as $F_n$ decreases below unity [1, 3, 43]. The "quantum limit" of a lightwave communication system should therefore more properly be designated as the "shot-noise limit."

The use of photon-number-squeezed light in visual science [5] could serve to clarify the functioning of ganglion cells in the mammalian retina. These cells transmit signals to higher visual centers in the brain via the optic nerve. In response to light, the ganglion cell generates a neural signal that takes the form of a sequence of nearly identical electrical events occurring along the time axis. The statistical nature of this neural signal is generally assumed to be governed by two nonadditive elements of stochasticity: the incident photons (which are Poisson-distributed in all experiments to date) and a randomness intrinsic to the cell itself [44]. If the statistical fluctuations of the photons could be controlled by exciting the retina with photon-number-squeezed light, the essential nature of the randomness intrinsic to the cell could be isolated and unambiguously determined. The use of photon-number-squeezed light as a stimulus in visual psychophysics experiments could also be helpful in clarifying the nature of seeing at threshold [5].

## APPENDIX GENERATION OF PHOTON-NUMBER-SQUEEZED AND ANTIBUNCHED LIGHT FROM INDEPENDENT RADIATORS

Consider an arbitrary (in general non-Poisson) excitation point process. Let each event of this process $\{t_1, t_2, \ldots, t_k, \ldots\}$ initiate a statistically independent and identical emission, so that the radiated light is the superposition of these emissions [12]. Even though the individual emissions typically take the form of pulses lasting a short time, and are therefore nonstationary, the overall radiation is stationary because of the assumed stationarity of the excitation process.

### Characterization of the Excitation Point Process

Two important descriptors of a stationary point process are the rate $\mu$ (events per unit time) and the rate of coincidence $\mu^2 g_e^{(2)}(\tau)$ of pairs of events at times separated by $\tau$. These descriptors are not sufficient to characterize an arbitrary point process completely [45, 46]; in general knowledge of the probability of multicoincidences of events at $k$ points, for $k = 1, 2, \ldots, \infty$, is required. If $m$ is the number of events that occur in a time interval $[0, T]$, then its mean is

$$\langle m \rangle = \mu T \tag{12.A1}$$



and its Fano factor (ratio of variance to mean) is

$$F_m(T) \equiv \frac{\mathrm{Var}(m)}{\langle m \rangle} = 1 + \frac{\langle m \rangle}{M_e} \tag{12.A2}$$

where

$$M_e^{-1} = \left(\frac{2}{T}\right) \int_0^\infty \left(1 - \frac{\tau}{T}\right) \left[g_e^{(2)}(\tau) - 1\right] d\tau \tag{12.A3}$$

The simplest example is the Poisson point process, for which $g_e^{(2)}(\tau) = 1$ and $F_m(T) = 1$. If $g_e^{(2)}(0) < 1$, the excitation process is said to be antibunched or anticorrelated, whereas if $g_e^{(2)}(0) > 1$ it is said to be bunched or correlated. The characteristic time associated with the function $[g_e^{(2)} - 1]$ is denoted $\tau_e$. Similarly, if $F_m(T) < 1$, the excitation counts are said to be sub-Poisson (for this counting time $T$), whereas if $F_m(T) > 1$, the counts are said to be super-Poisson. The Poisson point process has neither memory nor aftereffects.

For the self-exciting point process (SEPP), on the other hand, the probability of occurrence of an event at a particular time depends on the times and numbers of previous occurrences [46]. Renewal point processes (RPPs) form an important subclass of SEPPs for which the rate $\mu$ and the normalized coincidence rate $g_e^{(2)}(\tau)$ do characterize the process completely [45]. These are processes for which the interevent time intervals are statistically independent and identically distributed. The following are important examples of renewal point processes that exhibit antibunched events and sub-Poisson counts:

1. *The Gamma-$\mathcal{N}$ Process.* This process is obtained from a Poisson process by decimation, that is, by selecting every $\mathcal{N}$th event and discarding all others [45, 47], as illustrated in Figure 12.1*b* for $\mathcal{N} = 2$. The process is so named because the interevent time distribution $P(\tau)$ is a gamma distribution of order $\mathcal{N}$. For the particular case when $\mathcal{N} = 2$, it turns out that [12]

$$g_e^{(2)}(\tau) = 1 - \exp(-4\mu|\tau|) \tag{12.A4}$$

$$F_m(T) \approx \tfrac{1}{2} \tag{12.A5}$$

2. *The Nonparalyzable Dead-Time-Modified Poisson Process.* This process is obtained from a Poisson process by deleting events that fall within a specified dead time $\tau_d$ following the registration of an event [45–51]. It is

characterized by [12]

$$g_e^{(2)}(\tau) = \frac{1}{\mu}\sum_{l=1}^{\infty}\frac{[\lambda(\tau - l\tau_d)]^{l-1}}{(l-1)!}\exp[-\lambda(\tau - l\tau_d)]U(\tau - l\tau_d) \quad (12.A6)$$

$$F_m(T) \approx (1 - \mu\tau_d)^2 \quad (12.A7)$$

with

$$\lambda = \frac{\mu}{1 - \mu\tau_d} \quad (12.A8)$$

where $U(t)$ is the unit step function, $\lambda$ is the initial rate of the process, and $\mu$ is the rate after dead-time modification. [Equation (12.A6) replaces Eq. (3.43) in Ref. 1, which has a typographical error.] Its interevent-time density function is a decaying exponential function displaced to the minimum permissible interevent time $\tau_d$.

Another example is a pulse train with random time of initiation [12, 52].

**Photon Statistics for Emissions at Antibunched Times**

When the underlying excitation process has known rate $\mu$ and normalized coincidence rate $g_e^{(2)}(\tau)$, but is otherwise arbitrary, what can be said about the statistics of the radiation? Because of their finite lifetime, emissions overlap and interfere. To determine their bunching properties it is necessary to know not only the rate of coincidence of the excitation process at pairs of time instants but also the coincidence rates at triple points, and so on. If such information is not available, the bunching properties of the superposed radiation cannot be determined.

However, in the limit in which the counting time $T$ is much longer than the lifetime $\tau_p$ of the individual emissions, interference has a negligible effect on the total number of collected photocounts. The total number of photons $n$ is then simply the sum of the number of photons emitted *independently* by the individual emissions. If $m$ is the number of emissions and $\alpha_k$ is the number of photoevents associated with the $k$th emission, then $n = \sum_{k=1}^{m}\alpha_k$. Using the fact that the $\{\alpha_k\}$ are statistically independent and identical, it is not difficult to show that the mean and variance of $n$ are

$$\langle n\rangle = \langle\alpha\rangle\langle m\rangle \quad (12.A9)$$

$$\mathrm{Var}(n) = \langle\alpha\rangle^2\,\mathrm{Var}(m) + \langle m\rangle\mathrm{Var}(\alpha) \quad (12.A10)$$



from which it follows that the corresponding Fano factors are related by

$$F_n = \langle\alpha\rangle F_m + F_\alpha \quad (12.A11)$$

or

$$F_n = 1 + [F_\alpha - 1 + \langle\alpha\rangle] + \langle\alpha\rangle(F_m - 1) \quad (12.A12)$$

Equation (12.A10) is known as the *cascade variance formula* [53–55].

Equation (12.A12) shows that the Fano factor comprises three contributions. The first term is that of a Poisson process. The second term (in square brackets) represents excess noise due to randomness in the number of photons per emission (if $\alpha = 1$, then $F_\alpha = 0$ and it vanishes). The third term admits the possibility of noise reduction due to anticorrelations in the excitation process. This term vanishes if the excitation process is Poisson (since $F_m = 1$), whereupon Eq. (12.A11) assumes the well-known form

$$F_n = \langle\alpha\rangle + F_\alpha \quad (12.A13)$$

We now consider an example in which each of the individual emissions is described by a one-photon number state (i.e., single-photon emissions with $\alpha = 1$). This corresponds to $\langle\alpha\rangle = 1$ and $F_\alpha = 0$, from which Eq. (12.A11) yields

$$F_n = F_m \quad (12.A14)$$

This is to be expected. For single-photon emissions, the number of photons counted over a long time interval is approximately equal to the number of excitations (assuming there are no losses). If the excitation point process is sub-Poisson, the photons will also be sub-Poisson. It is of interest to note that we need not go outside the domain of linear (one-photon) optics to see such uniquely quantum-mechanical effects.

Equations (12.A11) and (12.A12) reveal the key to obtaining sub-Poisson photons from sub-Poisson excitations. In order to have $F_n < 1$, $F_\alpha$ must be $< 1$, as is apparent from Eq. (12.A11). Furthermore, a necessary condition for $F_n < 1$ is that $F_m < 1$ (because the term in square brackets in Eq. (12.A12) is nonnegative). It follows that for $F_n$ to be less than unity, both $F_\alpha$ and $F_m$ must be less than unity. Therefore, the generation of a stationary stream of sub-Poisson photons from a superposition of independent emissions requires that both the excitation process and the photons of the individual emissions be sub-Poisson.

Physical mechanisms that provide control of the excitation point process, and that are well described by the model presented here, have been discussed in Sections 12.3 and 12.4.

### Bunching/Antibunching Properties of Emissions Initiated' at Antibunched Times

Determination of the short-time behavior of the photoevents requires knowledge of the normalized photocoincidence rate $g^{(2)}(\tau)$. This is not possible unless the excitation point process is completely specified (higher-order multicoincidence rates specified). Teich et al. [12] examined this problem under the assumption that the excitation point process is a renewal point process. Using the assumption of single-mode individual emissions, they showed that

$$g^{(2)}(\tau) = 1 + |g^{(1)}(\tau)|^2 + \left(\frac{1}{\mu\tau_p}\right)\bar{g}^{(2)}(\tau) + r(\tau) \quad (12.A15)$$

The first three terms on the right-hand side of Eq. (12.A15) emerge from a Poisson excitation process. The fourth term, which is given by

$$r(\tau) = \int_0^\infty \psi(\tau, t)\left[g_e^{(2)}(t) - 1\right] dt \quad (12.A16)$$

with

$$\psi(\tau, t) = \int_0^\infty \left[I_0(t')I_0(t' + \tau - t) + V_0^*(t')V_0(t' + \tau) \times V_0^*(t + t')V_0(t + t' + \tau)\right] dt' \quad (12.A17)$$

represents the effects of deviation of the excitation process from Poisson. When the excitation point process is antibunched, this term is negative, thereby introducing anticorrelations into the photon process. If it is sufficiently strong, it can counterbalance the bunching effects due to wave interference [second term in Eq. (12.A15)] and due to the randomness of the individual emissions [third term in Eq. (12.A15)].

With the availability of Eq. (12.A15), the Fano factor for the photon counts in a time interval of arbitrary duration can be determined. The result can be put in the form [12]

$$F_n(T) = 1 + \frac{\langle n\rangle}{M} + \frac{F_\alpha(\infty) - 1 + \langle\alpha\rangle}{\mathscr{M}} + \frac{\langle n\rangle}{\mathscr{M}'} \quad (12.A18)$$

where $M$, $\mathscr{M}$, and $\mathscr{M}'$ are degrees-of-freedom parameters, the latter associated with the term $r(\tau)$. The parameter $\mathscr{M}'$ depends, in a complex way, on the relation between the counting time $T$, the emission lifetime $\tau_p$, and the excitation point process memory time $\tau_e$ (which is the width of the function $[g_e^{(2)}(\tau) - 1]$). For counting times that are long ($T \gg \tau_p, \tau_e$), however, it turns out that $M = \infty$ and wavelike (interference) noise is washed out; $\mathscr{M} = 1$ so that the role of noise in the individual emissions is enhanced; and $\mathscr{M}'$ is given by the degrees-of-freedom parameter for the excitation process $M_e$ given in Eq. (12.A3). It then follows that Eq. (12.A18) reduces to Eq. (12.A12), which was directly obtained by use of the cascade variance formula.



## ACKNOWLEDGMENT

This work was supported in part by the Joint Services Electronics Program through the Columbia Radiation Laboratory.

## REFERENCES

1. M. C. Teich and B. E. A. Saleh, "Photon bunching and antibunching," in *Progress in Optics*, Vol. 26, E. Wolf, ed., North-Holland, Amsterdam, 1988, pp. 1–104.
2. M. C. Teich and B. E. A. Saleh, *Quantum Opt.* **1**, 153 (1989); *Phys. Today* **43** (6), 26 (1990).
3. B. E. A. Saleh and M. C. Teich, *Phys. Rev. Lett.* **58**, 2656 (1987).
4. Y. Yamamoto and H. A. Haus, *Rev. Mod. Phys.* **56**, 1001 (1986).
5. M. C. Teich, P. R. Prucnal, G. Vannucci, M. E. Breton, and W. J. McGill, *Biol. Cybern.* **44**, 157 (1982).
6. R. E. Slusher, L. W. Hollberg, B. Yurke, J. C. Mertz, and J. F. Valley, *Phys. Rev. Lett.* **55**, 2409 (1985).
7. L.-A. Wu, M. Xiao, and H. J. Kimble, *J. Opt. Soc. Am. B* **4**, 1465 (1987).
8. R. Loudon and P. L. Knight, *J. Mod. Opt.* **34**, 709 (1987).
9. L. Mandel, *Phys. Rev. Lett.* **49**, 136 (1982).
10. Y. Yamamoto, S. Machida, N. Imoto, M. Kitagawa, and G. Björk, *J. Opt. Soc. Am. B* **4**, 1645 (1987).
11. Y. Yamamoto and S. Machida, Chapter 11, this volume.
12. M. C. Teich, B. E. A. Saleh, and J. Peřina, *J. Opt. Soc. Am. B* **1**, 366 (1984).
13. M. C. Teich and B. E. A. Saleh, *Opt. Lett.* **7**, 365 (1982).
14. B. E. A. Saleh, D. Stoler, and M. C. Teich, *Phys. Rev. A* **27**, 360 (1983).
15. B. E. A. Saleh and M. C. Teich, *Proc. IEEE* **70**, 229 (1982).
16. M. C. Teich, *Appl. Opt.* **20**, 2457 (1981).
17. R. Short and L. Mandel, *Phys. Rev. Lett.* **51**, 384 (1983).
18. M. C. Teich, B. E. A. Saleh, and D. Stoler, *Opt. Commun.* **46**, 244 (1983).
19. M. C. Teich, B. E. A. Saleh, and T. Larchuk, "Observation of sub-Poisson Franck–Hertz light at 253.7 nm," in *Digest XIII Int. Quant. Electron. Conf.*, Anaheim, CA, 1974 (Optical Society of America, Washington, DC, 1984), Paper PD-A6.

20. M. C. Teich and B. E. A. Saleh, *J. Opt. Soc. Am. B* **2**, 275 (1985).
21. S. K. Srinivasan, *Nuovo Cimento* **38**, 979 (1965).
22. S. K. Srinivasan, *Opt. Acta* **33**, 207 (1986).
23. M. C. Teich, F. Capasso, and B. E. A. Saleh, *J. Opt. Soc. Am. B* **4**, 1663 (1987).
24. S. Sze, *Physics of Semiconductor Devices*, 1st ed., Wiley, New York, 1969, p. 421, Eq. (95).
25. M. A. Lampert and A. Rose, *Phys. Rev.* **121**, 26 (1961).
26. M. A. Nicolet, H. R. Bilger, and R. J. J. Zijlstra, *Phys. Stat. Sol.* **B70**, 9 (1975).
27. M. A. Nicolet, H. R. Bilger, and R. J. J. Zijlstra, *Phys. Stat. Sol.* **B70**, 415 (1975).
28. P. Filipowicz, J. Javanainen, and P. Meystre, *Phys. Rev. A* **34**, 3077 (1986).
29. Y. Yamamoto, S. Machida, and O. Nilsson, *Phys. Rev. A* **34**, 4025 (1986).
30. S. Machida, Y. Yamamoto, and Y. Itaya, *Phys. Rev. Lett.* **58**, 1000 (1987).
31. S. Machida and Y. Yamamoto, *Phys. Rev. Lett.* **60**, 792 (1988).
32. D. F. Smirnov and A. S. Troshin, *Opt. Spektrosk.* **59**, 3 (1985) [transl. in *Opt. Spectrosc.* (USSR) **59**, 1 (1985)].
33. J. E. Carroll, *Opt. Acta* **33**, 909 (1986).
34. J. G. Walker and E. Jakeman, *Proc. Soc. Photo-Opt. Instrum. Eng.* **492**, 274 (1985).
35. S. Machida and Y. Yamamoto, *Opt. Commun.* **57**, 290 (1986).
36. Y. Yamamoto, N. Imoto, and S. Machida, *Phys. Rev. A* **33**, 3243 (1986).
37. J. H. Shapiro, M. C. Teich, B. E. A. Saleh, P. Kumar, and G. Saplakoglu, *Phys. Rev. Lett.* **56**, 1136 (1986).
38. J. H. Shapiro, G. Saplakoglu, S.-T. Ho, P. Kumar, B. E. A. Saleh, and M. C. Teich, *J. Opt. Soc. Am. B* **4**, 1604 (1987).
39. F. Capasso and M. C. Teich, *Phys. Rev. Lett.* **57**, 1417 (1986).
40. B. E. A. Saleh and M. C. Teich, *Opt. Commun.* **52**, 429 (1985).
41. F. Capasso, K. Mohammed, and A. Y. Cho, *Appl. Phys. Lett.* **48**, 478 (1986).
42. P. R. Tapster, J. G. Rarity, and J. S. Satchell, *Europhys. Lett.* **4**, 293 (1987).
43. K. Yamazaki, O. Hirota, and M. Nakagawa, *Trans IEICE Japan* **71**, 775 (1988).
44. B. E. A. Saleh and M. C. Teich, *Biol. Cybern.* **52**, 101 (1985).
45. D. R. Cox, *Renewal Theory*, Methuen, London, 1962.
46. D. L. Snyder, *Random Point Processes*, Wiley, New York, 1975.
47. E. Parzen, *Stochastic Processes*, Holden-Day, San Francisco, 1962.
48. L. M. Ricciardi and F. Esposito, *Kybernetik* (*Biol. Cybern.*) **3**, 148 (1966).
49. J. W. Müller, *Nucl. Instrum. Meth.* **117**, 401 (1974).
50. B. I. Cantor and M. C. Teich, *J. Opt. Soc. Am.* **65**, 786 (1975).
51. M. C. Teich and G. Vannucci, *J. Opt. Soc. Am.* **68**, 1338 (1978).
52. R. Loudon, *Rep. Progr. Phys.* **43**, 913 (1980).
53. W. Shockley and J. R. Pierce, *Proc. IRE* **26**, 321 (1938).
54. L. Mandel, *Brit. J. Appl. Phys.* **10**, 233 (1959).
55. R. E. Burgess, *J. Phys. Chem. Solids* **22**, 371 (1961).